Preprints of the 21st IFAC World Congress (Virtual)
Berlin, Germany, July 12-17, 2020

An Underwater Quadrotor Control with Wave-disturbance Compensation by a UKF

T. Ohhira * **A. Kawamura** * **A. Shimada** ** **T. Murakami** *

* *Graduate School of Science and Technology, Keio University, 3-14-1, Hiyoshi, Kohoku-ku, Yokohama, Kanagawa, 223-8522 JAPAN (e-mail: {ohhira, kawamura} @sum.sd.keio.ac.jp, mura@sd.keio.ac.jp).*
** *College of Engineering and Design, Shibaura Institute of Technology, Tokyo, JAPAN (e-mail: ashimada@sic.shibaura-it.ac.jp)*

Abstract: This paper proposes an unscented Kalman filter (UKF) with disturbance estimation for an underwater quadrotor control system by utilizing backstepping control. Autonomous underwater vehicles (AUVs) have been attracted attention to scientific and commercial applications. The tasks in those applications are such as surveys and inspections for various objects underwater in narrow space. In this study, a quadrotor type robot, in which high-performance results are obtained for aerial application, is regarded as AUVs. The quadrotor robot is a smaller system than general AUVs and has suitable merits for work in a narrow place. On the other hand, since the quadrotor system is small and light in weight, it is more susceptible to underwater waves than conventional AUVs. Therefore, consideration of a technique to suppress or to reject the influences of the waves in the control systems is a must. This paper proposes a UKF system including a second-order model of input disturbance for estimating the influence of waves and an accurate quadrotor state simultaneously. Additionally, the disturbance estimation performance assists in make robustness as its estimated disturbance is rejected to actual disturbance. Finally, the usefulness of the proposed system is shown via simulations of position control for the underwater quadrotor affected by a wave effect model.

Keywords: Motion estimation, Kalman filters, Disturbance rejection, State observers, Autonomous vehicles, Adaptive control.

1. INTRODUCTION

Autonomous underwater vehicles (AUVs) have been put to practical use in image and acoustic observations and water quality surveys for submarine pipeline inspection, submarine map creation, and ecological surveys. In the near future, AUVs are expected to be utilized to inspect for the bottom of a ship and revetments in a narrow workspace. Conventionally, those tasks at harbors require a precision motion in a stationary state and a constrained space and are performed by remotely operated vehicles or a diver. Moreover, such work has a safety risk because the distance between the work object and the others such as seabed, revetments, and so on becomes close. Therefore, if the tasks can be automated by utilizing AUVs, work efficiency and safety can be improved. However, since the conventional AUVs are mainly intended for a survey in deep-sea, the AUVs are a large system that has a lot of batteries and actuators for long navigation time, Wunn et al. (2014); Paull et al. (2014); Maki et al. (2014). A quadrotor type robot, which can control its positions and gyrating angle by four actuators, is widely utilized as aerial robots, Madani and Benallegue. (2006); Bouabdallah et al. (2004). Additionally, it is a smaller system than AUVs and has suitable merits for work in a narrow place. On the other hand, the quadrotor system is a small shape and lightweight system, therefore, it can be easily assumed that the system is susceptible to a change in underwater waves than conventional AUVs. Furthermore, the quadrotor robots have strong nonlinearity and are underactuated systems, therefore, its control system considering those effects is required. A quadrotor control system utilized backstepping control was proposed, and good results had been obtained, Madani and Benallegue. (2006). Therefore, the quadrotor control system by backstepping control is utilized in this study. In order to realize backstepping control for the underwater quadrotor, accurate state estimation for positions, postures, and their velocities under the influence of disturbances with strong nonlinearity by unknown waves is a must. In conventional quadrotor control, Kalman filter (KF) techniques for nonlinear systems such as extended Kalman filter (EKF) and unscented Kalman filter (UKF), Julier et al. (2000), are often utilized as state observer. Moreover, UKF systems have a high-estimation performance for aerial quadrotor systems, Goslinski et al. (2013). However, when underwater tasks affected by unknown waves are considered, the state estimation by EKF or UKF is always affected by unknown disturbances.

Disturbance observer (DOB) techniques, which estimate unknown disturbances as input disturbances, are known for considering unknown disturbance. The DOB is assuming step-type disturbances, therefore, it is strongly subject

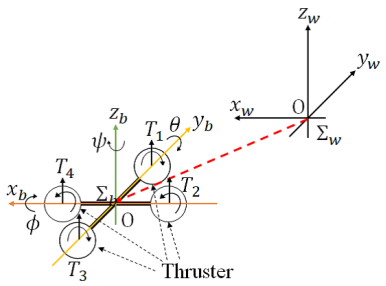

Fig. 1. Coordinate frame definition: Relationship of between time-invariant world coordinate frame(Σ_W) and body-COM coordinate frame (Σ_b)

to the influence of varying disturbances such as the waves. Therefore, this study attempts to integrate a second-order internal model of disturbance (sine-wave) into a UKF system for estimating an accurate quadrotor state considering the influence of waves as possible. In previous studies, linear KF-based DOB, Mitsantisuk et al. (2014), and linear KF with disturbance estimation, Ohhira and Shimada (2018) (previous work), have been proposed, and good results have been obtained for a step-type disturbance.

This study proposes an underwater quadrotor control system based on backstepping control utilizing a UKF considering the influence of underwater waves. The proposed UKF can consider and estimate the influence of waves as input disturbance estimates. Moreover, the UKF can perform state estimation considering the influence of unknown waves by utilizing the estimated disturbances. The disturbance estimates are utilized to suppress the influence of the wave by compensating for the input thrust like the conventional DOB. As a result, the backstepping control for the position and posture controls can be utilized the state estimates considering unknown wave disturbance. Finally, the proposed control system is verified by numerical simulation under the influence of designed wave effects, and its usefulness is shown via simulation results.

2. MODELING

In this paper, an underwater quadrotor, which has mounted diagonal four actuators to control position and posture, is utilized and its parameters are shown in Table 1. The world and body coordinate frames (Σ_W and Σ_b) have defined as in Fig. 1. Those coordinate frames are not general Right-hand coordination for treating the depth effect for a wave model. The position of the robot is defined from the origin position in the world coordinate frame that is fixed. It assumed that $z_w = 0$ is the position of the water surface. Consequently, the position and posture of the robot are handled as how much the robot moved from the origin of the world coordinate system.

2.1 Quadrotor

In this section, the mathematical modeling for the underwater quadrotor system based on Madani and Benallegue. (2006); Bouabdallah et al. (2004) is described. The state variables as $\boldsymbol{\zeta} = [x\ y\ z\ \phi\ \theta\ \psi]^T$ and the input thrust of each thruster as $\boldsymbol{T}[\mathrm{N}] = [T_1\ T_2\ T_3\ T_4]^T$ are defined. The motion equation of the quadrotor is given by,

$$\boldsymbol{M}\ddot{\boldsymbol{\zeta}} + \boldsymbol{D}(\dot{\boldsymbol{\zeta}}) + \boldsymbol{C}(\dot{\boldsymbol{\zeta}}) + \boldsymbol{G}(\boldsymbol{\zeta}) = \boldsymbol{E}(\boldsymbol{\zeta})\boldsymbol{B}_{tcm}\boldsymbol{T}. \quad (1)$$

Table 1. Specifications of quadrotor system

Notation [Unit]	Value	Explanation
m [kg]	1.3800	Mass of whole system
I_x [kg m^2]	0.8540	Moment of inertia about x-axis
I_y [kg m^2]	0.8540	Moment of inertia about y-axis
I_z [kg m^2]	0.9361	Moment of inertia about z-axis
D_m [N/ (m/s)]	0.0436	Coefficient of viscous friction for movement system
D_p [N/ (m/s)]	0.0082	Coefficient of viscous friction for posture system
F_m	0.0196	Attenuation coefficient proportional to square value on movement system
F_p	0.1037	Attenuation coefficient proportional to square value on posture system
d [m]	0.1090	Distance from COM to thruster
g [m/s^2]	9.8067	Gravity acceleration
$W(=-mg)$	-13.5323	Gravity constant
w_{rho} [kg m^3]	1000	Water density
V_r [m^2]	0.0011	Volume on x-y coordinates
$B(=V_r w_{rho} g)$	10.7866	Buoyancy constant
$G_z = (W - B)$	- 2.7457	Gravity and buoyancy constants
T_{lim} [N]	± 25	Output saturation of actuator

$\boldsymbol{M}$, $\boldsymbol{D}(\dot{\boldsymbol{\zeta}})$, $\boldsymbol{C}(\dot{\boldsymbol{\zeta}})$, $\boldsymbol{G}(\boldsymbol{\zeta})$, $\boldsymbol{E}(\boldsymbol{\zeta})$, and $\boldsymbol{B}_{tcm}$ denotes a mass-inertia matrix, a function of dynamic friction, Coriolis forces, buoyancy and gravity effects, an input transform function, and a thruster control matrix, respectively. Each variable is as given below: $\boldsymbol{M} = \mathrm{diag}(m, m, m, I_x, I_y, I_z)$,

$$\boldsymbol{D}(\dot{\boldsymbol{\zeta}}) = \begin{bmatrix} D_m\dot{x} + F_m|\dot{x}|\dot{x} \\ D_m\dot{+}F_m|\dot{y}|\dot{y} \\ D_p\dot{z} + F_p|\dot{z}|\dot{z} \\ D_p\dot{\phi} + F_p|\dot{\phi}|\dot{\phi} \\ D_p\dot{\theta} + F_p|\dot{\theta}|\dot{\theta} \\ D_m\dot{\psi} + F_m|\dot{\psi}|\dot{\psi} \end{bmatrix}, \quad \boldsymbol{C}(\dot{\boldsymbol{\zeta}}) = \begin{bmatrix} \dot{z}\dot{\theta} - \dot{y}\dot{\psi} \\ \dot{x}\dot{\psi} - \dot{z}\dot{\phi} \\ \dot{y}\dot{\phi} - \dot{x}\dot{\theta} \\ (I_z - I_y)\dot{\theta}\dot{\psi} \\ (I_x - I_z)\dot{\phi}\dot{\psi} \\ (I_y - I_x)\dot{\phi}\dot{\theta} \end{bmatrix},$$

$$\boldsymbol{G}(\boldsymbol{\zeta}) = \begin{bmatrix} -\sin\theta G_z \\ \sin\phi\cos\theta G_z \\ \cos\phi\cos\theta G_z \\ 0 \\ 0 \\ 0 \end{bmatrix}, \quad \boldsymbol{B}_{tcm} = \begin{bmatrix} 1 & 1 & 1 & 1 \\ -d & 0 & d & 0 \\ 0 & d & 0 & -d \\ d & -d & d & -d \end{bmatrix},$$

$$\boldsymbol{E} = \begin{bmatrix} \sin\theta\sin\psi + \cos\phi\sin\theta\cos\psi & 0\ 0\ 0 \\ -\sin\phi\cos\psi + \cos\phi\sin\theta\sin\psi & 0\ 0\ 0 \\ \cos\phi\cos\theta & 0\ 0\ 0 \\ 0 & 1\ 0\ 0 \\ 0 & 0\ 1\ 0 \\ 0 & 0\ 0\ 1 \end{bmatrix}.$$

$\boldsymbol{D}(\dot{\boldsymbol{\zeta}})$ includes the wave effect utilizing the Morison equation (ex. $F_m|\dot{x}|\dot{x}$ about x). This drag proportional to the square of momentary velocity represents the sum of an inertial force in phase with local wave acceleration underwater. The original Morison equation utilizes many complex parameters. Thus, this effect is designed by dividing and adding into inertial force $\boldsymbol{M}$ and drag force $\boldsymbol{D}(\dot{\boldsymbol{\zeta}})$ by utilizing the parameters $m, I_x, I_y, I_z, F_m, F_p$.

In addition, because the input thrust of each thruster can be independently controlled, the driving force (see the right side in (1)) is calculated by the controlled input thrusts via the $\boldsymbol{E}(\boldsymbol{\zeta})$ and $\boldsymbol{B}_{tcm}$.

$$\boldsymbol{E}(\boldsymbol{\zeta})\boldsymbol{B}_{tcm}\boldsymbol{T} = [\,U_x\ U_y\ U_z\ \tau_\phi\ \tau_\theta\ \tau_\psi\,]^T \quad (2)$$

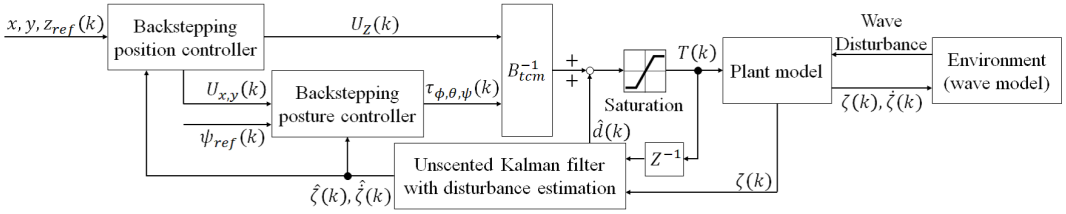

Fig. 2. Configuration diagram on the whole system of the backstepping controller and the DOB-based UKF

In the simulation, the $\boldsymbol{\zeta}$ is calculated by utilizing a double integral of (3).

$$\ddot{\boldsymbol{\zeta}} = \boldsymbol{M}^{-1}\{\boldsymbol{E}(\boldsymbol{\zeta})\boldsymbol{B}_{tcm}\boldsymbol{T} - (\boldsymbol{D}(\dot{\boldsymbol{\zeta}}) + \boldsymbol{C}(\dot{\boldsymbol{\zeta}}) + \boldsymbol{G}(\boldsymbol{\zeta}))\} \quad (3)$$

2.2 Underwater wave effect

In this section, a model for the effect of an underwater wave by utilizing the JONSWAP Spectrum, Hasselmann et al. (1973), is described. This spectrum can represent surface wave behavior. Thus, the influence model of underwater waves with respect to surface waves considering water depth is designed by this spectrum. In this study, the z-axis waves utilizing the JONSWAP Spectrum are considered, and the disturbances about the x and y axes are designed via $\boldsymbol{E}(\boldsymbol{\zeta})$. The underwater wave is calculated by the surface waves and the velocity and depth of the robot. The disturbances on the roll, pitch, and yaw angles are calculated by atan2 function with low-pass filter utilizing x, y and z disturbances. The result of the designed surface wave model is shown in Fig. 6. The results indicated that nonlinear and irregular disturbances are generated by the designed model.

3. PROPOSED CONTROL SYSTEM DESIGN

In this section, the proposed control system in detail is explained. The configuration diagram of the proposed system is shown in Fig. 2. In general, control systems for quadrotor robots have four main problems as an underactuated system, coupled motion, linear approximation error, and nonlinear control. This study utilizes backstepping control for controlling the quadrotor. This control method solves the problems of the underactuated system and nonlinear control. Besides, the lateral motion (x and y) of the quadrotor is coupled with two state variables. One is x-axis displacement (x) and pitch-angle (θ) and the other is y-axis displacement (y) and roll-angle (ϕ). Therefore, the reference design coping with the coupled motion adds in the control system (see (14)). Moreover, the remaining problem of the linear approximation error is solved by utilizing a UKF. Furthermore, since the proposed method compensates for the influence of waves, and the accurate state estimation is simultaneously realized by utilizing the proposed UKF.

3.1 Backstepping controller

This section explains the quadrotor control system by a backstepping control. The control system has designed by applying the Lyapunov stabilization theorem for each state variable in $\boldsymbol{\zeta}$. In order to design the backstepping control system, the new control variables $\boldsymbol{q}$ are defined by,

$$\boldsymbol{q} = \begin{bmatrix} q_1 = x & q_2 = \dot{x} & q_3 = y & q_4 = \dot{y} & q_5 = z & q_6 = \dot{z} \\ q_7 = \phi & q_8 = \dot{\phi} & q_9 = \theta & q_{10} = \dot{\theta} & q_{11} = \psi & q_{12} = \dot{\psi} \end{bmatrix}. \quad (4)$$

The $x\ (= q_1)$ is explained as an example. A tracking error variable of Z_1 for q_1 is defined by utilizing the reference value x_{ref}.

$$Z_1 = x_{ref} - q_1 \quad (5)$$

A positive-definite Lyapunov function by utilizing (5) is designed and is given by,

$$V(Z_1) = \frac{1}{2}Z_1^2. \quad (6)$$

Next, a derivative of (6) is derived by,

$$\frac{d}{dt}V(Z_1) = \frac{1}{2}\cdot\frac{d}{dt}Z_1^2 = Z_1(\dot{x}_{ref} - q_2). \quad (7)$$

If (7) is negative-definite function, (6) is a Lyapunov function. To realize stabling for Z_1, a pseudo-control input q_2 is derived and is given by,

$$q_2 = \dot{x}_{ref} + \alpha_1 Z_1. \quad (8)$$

The α_1 denotes the control parameter for stabilizing the q_1 and has a stabilizing condition $\alpha_1 > 0$. Next, (8) is substituted in (7) as,

$$\frac{d}{dt}V(Z_1) = Z_1\{\dot{x}_{ref} - (\dot{x}_{ref} + \alpha_1 Z_1)\} = -\alpha_1 Z_1^2. \quad (9)$$

Next, new value Z_2 regarding (9) is defined.

$$Z_2 = q_2 - \dot{x}_{ref} - \alpha_1 Z_1 \quad (10)$$

A Lyapunov function for stabilizing the whole system about the q_1 is derived by,

$$V(Z_1, Z_2) = \frac{1}{2}Z_1^2 + \frac{1}{2}(q_2 - \dot{x}_{ref} - \alpha_1 Z_1)^2. \quad (11)$$

Additionally, the differential function for (11) is given by,

$$\begin{aligned}\frac{d}{dt}V(Z_1, Z_2) = &-\alpha_1 Z_1^2 + Z_2(-G_z/m\sin q_9 + u_x/mU_z) \\ &-Z_2\{\ddot{x}_{ref} - \alpha_1(Z_2 + \alpha_1 Z_1) - Z_1\} \\ &-\alpha_1 Z_1^2, \end{aligned} \quad (12)$$

where, $u_x = \sin\theta\sin\psi + \cos\phi\sin\theta\cos\psi$ and $\ddot{x} = -G_z/m\sin q_9 + U_z \cdot u_x/m$ without friction term. The friction term in the underwater robot is a time-variant parameter, therefore, it is designed as the modeling error. The control input by utilizing (12) satisfies two conditions for $\ddot{x}_{ref} = 0$ and $\dot{V}(Z_1, Z_2) < 0$, and it is given by,

$$U_x = \frac{m}{U_z \cdot u_x}(Z_1 - \frac{G_z}{m}\sin q_9 - \alpha_1\{Z_2 + \alpha_1 Z_1\} - \alpha_2 Z_2). \quad (13)$$

α_2 is a stabilizing parameter for Z_2. Since other control input variables (U_y, U_z, τ_ϕ, τ_θ, τ_ψ) can be obtained in the same manner, its description is omitted.

The quadrotor system is an underactuated system. Specifically, the motion of the x simultaneously occurs with the motion of θ. The x can not control without the motion of the θ, that is, the x can control by controlling the θ. Hence, in order to control the x, the U_x is utilized as the angle reference for the θ. The angle reference is given by,

$$\theta_{ref} = \begin{cases} |U_x| & U_x > 0 \cap U_z > 0 \\ -|U_x| & U_x > 0 \cap U_z < 0 \\ -|U_x| & U_x < 0 \cap U_z > 0 \\ |U_x| & U_x < 0 \cap U_z < 0 \\ 0 & \text{(otherwise)} \end{cases} \tag{14}$$

Furthermore, the reference includes in with rotate motion ($\theta_{ref} > \pi/2$, and $\theta_{ref} < -\pi/2$). Therefore, the absolute value of the U_x is treated as the reference for the θ by utilizing a saturation function with ($-\pi/4 \leq \theta_{ref} \leq \pi/4$). The relationship between y and ϕ is handled in the same manner as x and θ.

3.2 UKF with disturbance estimation

The backstepping controller requires the full-state observation ($\boldsymbol{\zeta}$ and $\dot{\boldsymbol{\zeta}}$). In this study, it is assumed that the $\boldsymbol{\eta}(k) = \boldsymbol{\zeta}(k)$ with noise can be observed. In order to estimate the true $\boldsymbol{\zeta}$ and the $\dot{\boldsymbol{\zeta}}$, a nonlinear observer considering the influences of noise and disturbance simultaneously is a must. In addition, the state observer must consider the influences of waves affecting underwater robots. Therefore, the UKF, which has the potential to cope with the nonlinearity of the quadrotor and underwater wave simultaneously, is utilized as the state observer.

In this study, a UKF with a higher-order disturbance estimation function that can handle sine wave type disturbance and the effects of noise is proposed for the underwater quadrotor control. This method simultaneously estimates the state variables and the disturbance of the input thrust by the influence of the wave while handling the influences of the noise. If such UKF can be realized, the correct state estimation of nonlinear systems can be performed under the influences of disturbance and noise. The basic structure of the proposed UKF is based on Julier et al. (2000). The UKF design is not special, therefore, the internal model for designing UKF is only explained. This paper utilizes an internal model augmented by disturbance estimates. As the internal model for the UKF, an augmented model is designed by utilizing a second-order model of input disturbance. The second-order model of input disturbance is given by,

$$\boldsymbol{d}(k) = \boldsymbol{d}(k-1) + \delta \dot{\boldsymbol{d}}(k-1), \tag{15}$$

$$\dot{\boldsymbol{d}}(k) = \dot{\boldsymbol{d}}(k-1) + \delta \ddot{\boldsymbol{d}}(k-1). \tag{16}$$

$\boldsymbol{d}$ denotes the input disturbance vector, and $\delta = 0.01$s is a sampling time. The state variables augmented by the disturbance are given by,

$$\begin{aligned} \bar{\boldsymbol{\zeta}}(k) &= [\boldsymbol{\zeta}(k)\ \dot{\boldsymbol{\zeta}}(k)\ \boldsymbol{d}(k)\ \dot{\boldsymbol{d}}(k)\ \ddot{\boldsymbol{d}}(k)]^T \in \mathbb{R}^{24\times 1} \\ &= [x(k)\ y(k)\ z(k)\ \phi(k)\ \theta(k)\ \psi(k)... \\ &\quad \dot{x}(k)\ \dot{y}(k)\ \dot{z}(k)\ \dot{\phi}(k)\ \dot{\theta}(k)\ \dot{\psi}(k)... \\ &\quad d_{T_1}(k)\ d_{T_2}(k)\ d_{T_3}(k)\ d_{T_4}(k)... \\ &\quad \dot{d}_{T_1}(k)\ \dot{d}_{T_2}(k)\ \dot{d}_{T_3}(k)\ \dot{d}_{T_4}(k)... \\ &\quad \ddot{d}_{T_1}(k)\ \ddot{d}_{T_2}(k)\ \ddot{d}_{T_3}(k)\ \ddot{d}_{T_4}(k)]^T. \end{aligned} \tag{17}$$

Table 2. List of simulated systems

Symbol	Type of Kaman filter	Disturbance estimation
(a)	UKF	second-order (proposed)
(b)	EKF	second-order
(c)	UKF	zero-order
(d)	EKF	zero-order
(e)	UKF	none (conventional)
(f)	EKF	none (conventional)

An output equation is given by,

$$\boldsymbol{\eta}(k) = \boldsymbol{\zeta}(k) = \boldsymbol{C}\bar{\boldsymbol{\zeta}}(k) = \begin{bmatrix} \boldsymbol{I}^{\in\mathbb{R}^{6\times 6}} & \boldsymbol{0}^{\in\mathbb{R}^{6\times 18}} \end{bmatrix} \bar{\boldsymbol{\zeta}}. \tag{18}$$

The augmented system as the internal model is given by,

$$\bar{\boldsymbol{\zeta}}(k) = f(\boldsymbol{\zeta}(k-1), \boldsymbol{T}(k-1)) = \bar{\boldsymbol{\zeta}}(k-1) + \delta \begin{bmatrix} \hat{\dot{\boldsymbol{\zeta}}}(k-1) \\ \hat{\ddot{\boldsymbol{\zeta}}}(k-1) \\ \dot{\boldsymbol{d}}(k-1) \\ \ddot{\boldsymbol{d}}(k-1) \\ \boldsymbol{0}^{4\times 1} \end{bmatrix}. \tag{19}$$

The inputs translate from $\boldsymbol{T}(k-1)$ to $\boldsymbol{T}(k-1) + \hat{\boldsymbol{d}}(k-1)$, and $\hat{\ddot{\boldsymbol{\zeta}}}(k-1)$ is obtained by utilizing discretized (3). The proposed UKF utilizing this augmented system model can cope with a sine wave type disturbance in theory.

4. SIMULATION RESULTS

The performances of the proposed system were verified via numerical simulations in motion control for the underwater quadrotor. The initial state of the robot and the UKF are $\boldsymbol{\zeta}(0)$ =[0 0 -10 0 0 0], and the references for the state are set by $\boldsymbol{\zeta}_{ref}$ =[10 15 -10 0 0 0]. Moreover, the proposed system and multiple systems utilizing conventional KF methods with the same controller were compared. The compared methods are shown in Table 2. All systems can control the underwater quadrotor in theory because the backstepping control systems have the function of handling the disturbances by waves as the modeling error.

4.1 Parameter design

In a tune-up of the backstepping controller, a discrete-time linear quadratic regulator (DLQR) method was utilized to decide the controller parameters ($\alpha_1, ..., \alpha_{12}$). The weight matrices for tracking error $\boldsymbol{Q}_{LQR}$ and input $\boldsymbol{R}_{LQR}$ for DLQR were designed via trial and error in a simulation as ($\boldsymbol{Q}_{LQR} = \mathrm{diag}\{10^2, 10^2, 10^3, 4\times 10^3, 4\times 10^3, 5\times 10^4, 1, 1, 10^2, 10^3, 10^3, 5\times 10^2\}$) and ($\boldsymbol{R}_{LQR} = 10^3 \times \boldsymbol{I}^{6\times 6}$). The controller parameters obtained by DLQR are given by $\{\alpha_1, ..., \alpha_{12}\}$ = { 0.3152, 0.3152, 3.1285, 1.9756, 1.9756, 6.9341, 0.8908, 0.8908, 2.9469, 2.0775, 2.0775, 3.6262 }. In all simulations, the variances of the system W_s and sensor V_m, V_p are designed as ($W_s = 0.1$) and ($[V_m, V_p]$ = [0.1, 0.01]). The variance parameters on W_s, V_m, and V_p indicate a wave disturbance, a position sensor resolution, and angle sensor resolution, respectively. In the initial parameters for the UKF, the covariance matrices for estimation error $\boldsymbol{P}_0$, state variables $\boldsymbol{Q}_{ukf}$, and observed variables $\boldsymbol{R}_{ukf}$ are designed as $\boldsymbol{P}_0 = \mathrm{diag}(10^{-1}\cdot\boldsymbol{I}^{3\times 3}, 10^{-2}\cdot\boldsymbol{I}^{3\times 3}, 10\cdot\boldsymbol{I}^{3\times 3}, \boldsymbol{I}^{3\times 3}, 1\cdot\boldsymbol{I}^{4\times 4}, 10\cdot\boldsymbol{I}^{4\times 4}, 10^2\cdot\boldsymbol{I}^{4\times 4})$, $\boldsymbol{Q}_{ukf} = \mathrm{diag}(10^{-2}\cdot\boldsymbol{I}^{3\times 3}, 10^{-3}\cdot\boldsymbol{I}^{3\times 3}, \boldsymbol{I}^{3\times 3}, 10^{-1}\cdot\boldsymbol{I}^{3\times 3}, 5\cdot 10^5\cdot\boldsymbol{I}^{4\times 4}, 1/\delta\cdot 10^6\cdot\boldsymbol{I}^{4\times 4}, 1/\delta^2\cdot 10^6\cdot\boldsymbol{I}^{4\times 4})$, $\boldsymbol{R}_{ukf} =$

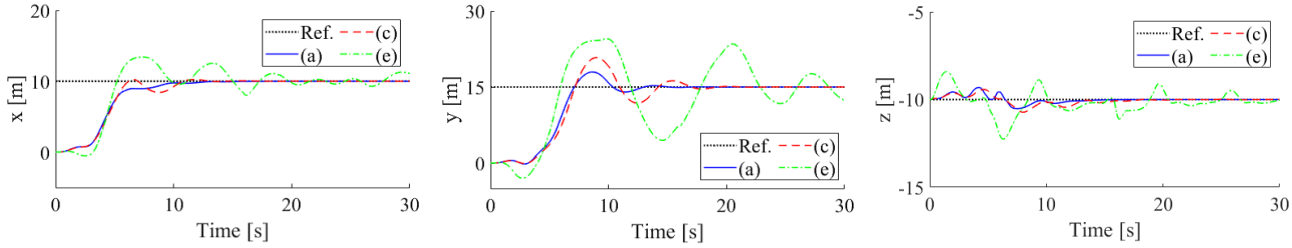

i). x ii). y iii). z

Fig. 3. Simulation (a, c, e): estimation results about position by UKF-based systems

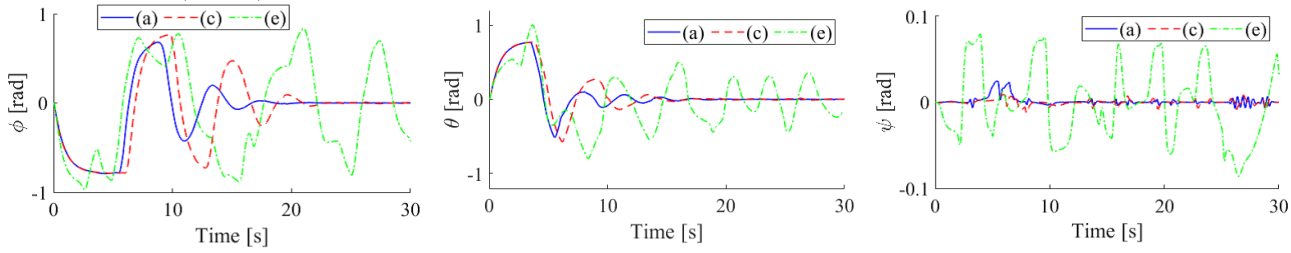

i). ϕ ii). θ iii). ψ

Fig. 4. Simulation (a, c, e): estimation results about posture by UKF-based systems

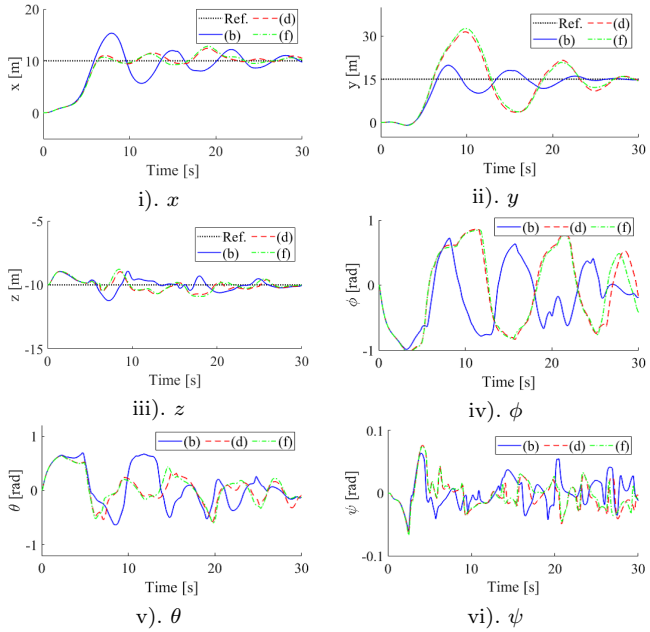

i). x ii). y iii). z iv). ϕ v). θ vi). ψ

Fig. 5. Simulation (b,d,f): EKF-based systems

diag$(V_m, V_m, V_m, V_p, V_p, V_p)$. These matrices were decided by trial and error via a simulation which considers the estimation speed on the disturbances and velocities. The estimation speed for the disturbance and the estimation accuracy for the velocity of the state can be adjusted by increasing the parameters $(5{\cdot}10^5{\cdot}\boldsymbol{I}^{4\times4}, 1/\delta{\cdot}10^6{\cdot}\boldsymbol{I}^{4\times4}, 1/\delta^2{\cdot}10^6\cdot\boldsymbol{I}^{4\times4})$ corresponding to the disturbance estimation in $\boldsymbol{Q}_{ukf}$. However, an excessive increase occurs noise into the state and the disturbance estimates.

4.2 Simulation verification

Figures 3 and 4 show the simulation results on the response values of position and posture by UKF-based systems and Figure 5 shows the simulation results by EKF-based systems. Furthermore, the surface wave utilized in all simulations is shown in Fig. 6(i). The disturbances regarding (a) for state variables generated by the surface wave model are shown in Fig. 6(ii). Additionally, Figure 7 illustrates the results for the disturbance estimation by zero/second-order model of the disturbance. Moreover, the results of the velocity estimation focusing on the ϕ correspond to y, which has the highest reference in the control system, is shown in Fig. 8.

From these simulation results, it is confirmed that the control variables in the UKF systems including disturbance estimation (a,c) can converge into the reference under the influences of unknown disturbance by the waves (see Figs. 3 – 5), and it can also be confirmed that the systems of (a) and (c) have a suppression function of disturbance and oscillation by unknown disturbance compared to other systems. In contrast, the EKF-based systems (b,d,f) and the general UKF system (e) can not converge into the reference within the simulation time and can not achieve the tracking control without oscillation owing to be affected by the wave disturbances. Additionally, it can confirm that the EKF-based backstepping controller has oscillation about the x, y, and z. This fact indicates that the UKF-based systems have an advantage for underwater quadrotor control than EKF systems.

Moreover, the results of the disturbance estimation shown in Fig. 7 indicates that the estimation performance for the disturbance by the UKF systems is better than the EKF systems. In addition, it can be seen that the system (a) utilizing the second-order model can estimate and suppress the high-frequency disturbance due to the underwater waves than the system (c) utilizing the zero-order model. In contrast, it can be confirmed that the performance of disturbance estimation by the EKF systems is not sufficient. In particular, from Fig. 7 (ii, iv), the EKF utilizing the zero-order model (d) can not handle the disturbance estimation, and the EKF utilizing the second-order model can not sufficiently estimate the disturbance by the waves. The main reason for differences in the results of the UKF and EKF comes from how to handle the

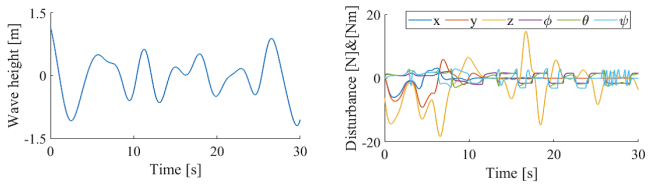

i). surface wave heigh ii). input distrubance (a)

Fig. 6. Simulation: wave disturbance

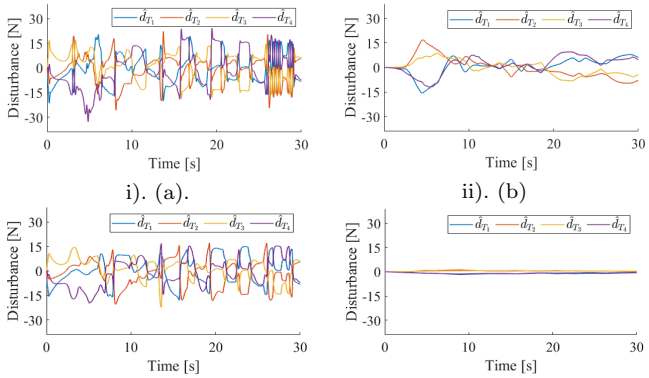

i). (a). ii). (b)

iii). (c) iv). (d)

Fig. 7. Simulation(a,b,c,d) : disturbance estimates

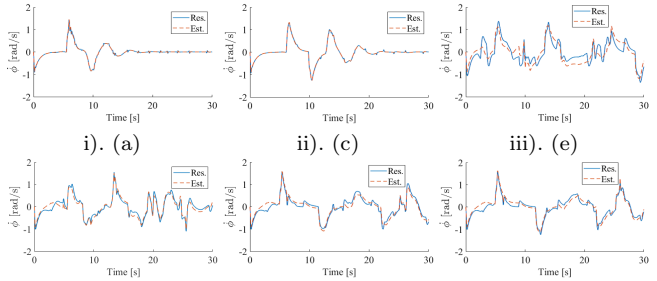

i). (a) ii). (c) iii). (e)

iv). (b) v). (d) vi). (f)

Fig. 8. Simulation : velocity estimation $\dot{\phi}$

system noise. The UKF systems handle the system noise as covariance for the state variables, therefore, the UKF systems can directly handle the state and disturbance estimations considering the uncertainty of the disturbance by designing the suitable system noise. On the other hand, the EKF systems treat the system noise as covariance for the input thrust, therefore, the EKF systems can not directly consider the uncertainty of the disturbance on the state variables. Furthermore, the handling method of the nonlinearity of the internal model is also different. It can be confirmed that those performances for suppressing unknown wave disturbances are obtained by utilizing the proposed UKF with disturbance estimation. Additionally, from these results, it confirmed that DOB-based UKF systems have high adaptive performances for wave disturbances. In particular, in Figs. 3(i, ii) and 4(i, ii), it can be confirmed that the proposed method with the use of the second-order model suppresses the oscillation and overshoot by the underwater wave than other systems. Similarly, from Fig. 8, it can simultaneously be confirmed that the velocity estimation by the UKF with disturbance estimation is better than the other systems. From these simulation results, the effectiveness and feasibility of the proposed system in underwater environments are shown.

5. CONCLUSION

This paper proposed the UKF with disturbance estimation for the underwater quadrotor control method considering the influences of unknown waves and verified its effectiveness by the simulations. This paper showed the usefulness of the UKF including the second-order model of disturbance. Additionally, the potential that the proposed system can improve the control performances of model-based control systems by estimation of the internal model augmented by the disturbance is shown. However, the sea wave model designed in this study is not perfect. Therefore, additional verification via experimental by actual quadrotor robot is required.

ACKNOWLEDGEMENTS

This work was supported in part by KEIRIN JKA(2020M-127).

REFERENCES

Bouabdallah, S., Murrieri, P., and Siegwart, R. (2004). Design and control of an indoor micro quadrotor. *Proc. of IEEE International Conference on Robotics and Automation*, pages 4393–4398.

Goslinski, J., Giernacki, W., and Gardecki, S. (2013). Unscented Kalman Filter for an orientation module of a quadrotor mathematical model. *Proc. of 9th Asian Control Conference (ASCC)*.

Hasselmann, K., Barnett, T.P., Bouws, E., et al. (1973). Measurements of wind-wave growth and swell decay during the Joint North Sea Wave Project (JONSWAP). *Dtsch Hydrogr. Z. Suppl.*, 12(A8) pages 1–95.

Julier, S., Uhlmann, J., and Durrant-Whyte, H. F. (2000). A new method for the nonlinear transformation of means and covariances in filters and estimators. *IEEE Transactions on Automatic Control*, Vol.45, No.3, pages 477–482.

Madani, T., and Benallegue, A. (2006). Backstepping control for a quadrotor helicopter. *Proc. of IEEE/RSJ International Conference on Intelligent Robots and Systems*, pages 3255–3260.

Maki, T., Sato, Y., Matsuda, T., Shiroku, R., and Sakamaki, T. (2014). AUV Tri-TON 2: An intelligent platform for detailed survey of hydrothermal vent fields. *Proc. of 2014 IEEE/OES Autonomous Underwater Vehicles (AUV)*, pages 4393–4398.

Mitsantisuk, C., Ohishi, K., and Katsura S. (2014). Estimation of action/reaction forces for the bilateral control using Kalman filter. *IEEE Transactions on Industrial Electronics*, Vol.59, No.11, pages 4383–4393.

Ohhira, T., and Shimada, A. (2018). Movement control based on model predictive control with disturbance suppression using Kalman filter including disturbance estimation. *IEEJ Journal of Industry Applications*, Vol.7, No.5, pages 387–395.

Paull, L., Saccdi, S., Seo, M., and Li, H. (2014). AUV Navigation and Localization: A Review. *IEEE J. Ocean. Eng.*, Vol.39, No.1, pages 131–149.

Wynn, R. B., et al, (2014). Autonomous Underwater Vehicles (AUVs): Their past, present and future contributions to the advancement of marine geoscience. *Marine Geology*, Vol. 352, pages 451–168.